Supplementary Material

S1: Thermodynamical argument:

Gas bubble surrounded by intergranular capillary-held water and a thick water film

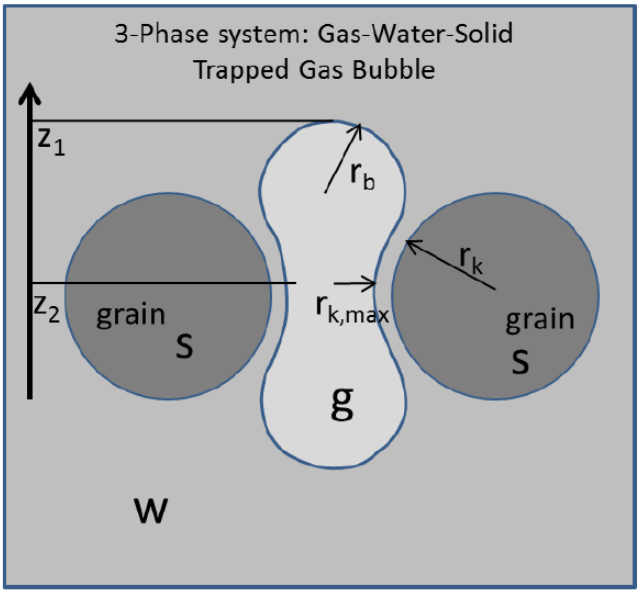

Figure S1 Trapped gas bubble surrounded by intergranular capillary-held water and a thick water film.

(i) Assumption: The glass beads sediment is completely surrounded by intergranular capillary-held water and a thick, coherent (= continous) water film (normal water phase with same density and viscosity as the bulk water phase).

(ii) For a stable trapped gas bubble shown in Fig. S1 the gas pressure inside the bubble has to be constant:

$$p_g(z_1) = p_g(z_2)\ . \tag{S1}$$

With

$$p_g(z) = p_c(z) + \rho_w g \cdot z, \tag{S2}$$

one obtains the *thermodynamic stability condition*:

$$p_c(z_2) - p_c(z_1) = p_c(z) + \rho_w g(z_1 - z_2) \cong \rho_w g \cdot r_k \geq 0, \tag{S3}$$

where the equality sign stands for g = 0, i.e. for a horizontal gas bubble and r_k denotes the grain radius.

(iii) Calculation of the capillary pressure by the Young-Laplace equation yields:

$$p_c(z_1) = 2\gamma_{g,w}/r_b \cong 2\gamma_{g,w}/r_{k,max} \tag{S4a}$$

$$p_c(z_2) = \gamma_{g,w}\,(1/r_{k,max} - 1/r_k) \qquad \text{(S4b)}$$

(r_b – bubble radius, $\gamma_{g,w}$ – surface tension or excess free energy).

(iii) Inserting (S4) into (S3) yields a negative expression for the difference of the capillary pressures and therfore a contradiction to assumption (i), namely:

$$p_c(z_2) - p_c(z_1) = -\gamma_{g,w}/r_k\,(1 + 1/\xi_{max}) < 0 \qquad \text{(S5)}$$

with $r_{k,max} = \xi_{max} \cdot r_k$.

(iv) Conclusion: The result (S5) can be interpreted in two ways: (i) If there exists a *stable* trapped gas bubble with $r_b > r_{k,max}$ a surrounding thick water film is thermodynamically not possible. (ii) If there exists a thick water film, then trapped gas bubbles with $r_b > r_{k,max}$ are thermodynamically *unstable*. Since about 50% of all trapped gas bubbles (see Table S1) have a radius larger than $r_{k,max}$ and the trapped gas bubbles exhibit a negative curvature shown in Fig. 4, a complete wetting of the whole sediment by intergranular capillary-held water and thick water films is thermodynamical not possible.

(v) Disjoining pressure and augmented Young-Laplace equation

If we add an additional repulsive disjoing pressure to the capillary pressure at z_2 we obtain the augmented Young-Laplace equation:

$$\tilde{p}_c(z_2) = p_c(z_2) + \Pi(h), \qquad \text{(S6)}$$

where $\Pi(h)$ denotes the short-ranged disjoining pressure, and h the film thickness. Inserting (S6) into (S3) yields:

$$\Pi(h_{equ}) = \frac{\gamma_{g,w}}{r_k}\left(1 + \frac{1}{\xi_{max}}\right) + \rho_w g r_k \cong 400\ Pa\ , \qquad \text{(S7)}$$

with $\gamma_{g,w}$ = 73 mN/m, r_k = 0.5 mm, and ξ_{max} = 0.6 (see Geistlinger et al., 2006). Physically, (S7) means that a new mechanical equilibrium has been established at the gas-water interface for a disjoining pressure of about 400 Pa (see Fig. 3 Disjoining pressure isotherm). In order to obatain a rough estimate of the relevant scale of the equilibrium film thickness h_{equ} we calculate the disjoining pressure by van der Waals forces only (for details see Safran, 1997):

$$\Pi_{vdW}(\mathrm{h}) = \frac{-A_{123}}{6\pi h^3}\ , \qquad \text{(S8)}$$

with the Hamaker constant $A_{123} = -1.3 \times 10^{-20}$ J (French, 2000). Inserting (S8) into (S7) yields the relevant scale for the equilibrium film thickness of about 12 nm, i.e. the new equilibrium leads to a stable thin adsorbed water film.

(viii) What about incoherent, *discontinous thick water films*? They are thermodynamically possible?

According to the *Second Law of Thermodynamics* the system at thermodynamic equilibrium trys always to find it minimal *Free Energy*. We compare the *Free Energy* of a thick film (thickness = δ) that covers a grain and a triangular pendular ring (inner radius = 0, outer radius = r_a). The boundary condition of equal phase volume yields:

$$r_a(\delta) = \sqrt[3]{\frac{4}{\sqrt{3}} \cdot \{(r_k + \delta)^3 - {r_k}^3\}} \qquad \text{(S6)}$$

The difference of the *Free Energy* considering only the gas-water *Excess Free Energy* is

$$\Delta F = \gamma_{g,w} \cdot 4\pi\{(r_k + \delta)^2 - r_a^2(\delta)/\sqrt{3}\}. \qquad \text{(S7)}$$

Calculating ΔF for r_k = 0.5 mm (1mm-GBS), yields for film thicknesses $\delta < r_k$ positive values for ΔF. Hence, the thick film will draw back to a pendular ring, since its *Free engergy* is smaller, i.e. incoherent thick films that cover a grain are thermodynamically not stable!

S2: Thermodynamics of Interfaces: Calculation of the Free Energy

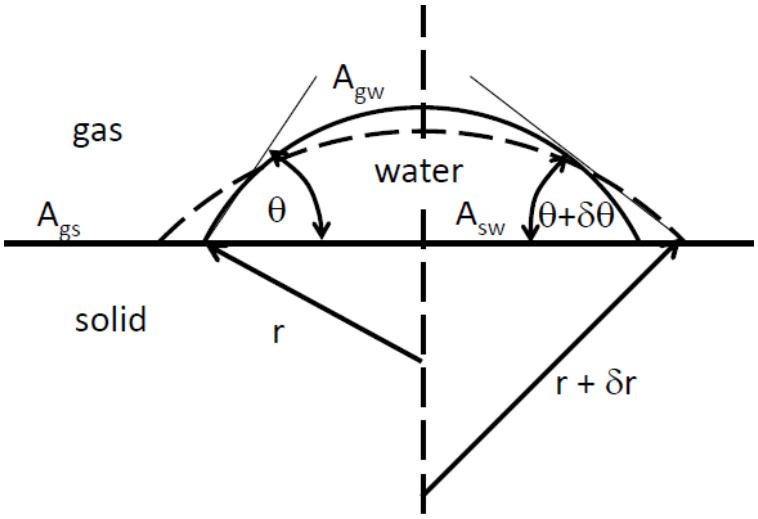

Figure S2 Spreading of a thick water film (circular cap) from contact angle θ to θ + δθ .

(i) We consider a spherical curved water film with a circular-cap geometry shown in Fig. S2 with the following boundary lines (or 2D-interfaces):

$$A_{g,w} = 2r\theta, \qquad \text{(S9)}$$

$$A_{s,w} = 2r \cdot \sin(\theta), \qquad \text{(S10)}$$

and the area or 2D-volume of the water phase:

$$V_w = r^2(\theta - \sin(2\theta)/2), \qquad \text{(S11)}$$

(ii) An increase of the g-w-interface by $dA_{g,w}$, will increase the *Free Energy* of the system by

$$dF_{g,w} = \gamma_{g,w} \cdot dA_{g,w}$$

and (S12)

$$dF_{s,w} = \gamma_{s,w} \cdot dA_{s,w},$$

where γ [Nm/m] denotes the *Excess Free Energy*. Physically, the increase is caused by the loss of binding energy, i.e. water molecules from the phase volume (binding energy ~ 12 ε for face-centered coordination) lose ~ 6 ε of their binding energy (= negative energy!), if they reach the surface.

(iii) The system wins binding energy, if the g-s-interface $dA_{s,g}$ is decreased, since water molecules in general are stronger bounded at the solid surface than gas molecules, i.e.:

$$dF_{s,g} = -\gamma_{s,g} \cdot |dA_{s,g}| . \quad \text{(S13)}$$

(iv) The system at thermodynamic equilibrium possesses a minimal *Free Energy*, therefore holds:

$$dF = \gamma_{g,w} \cdot dA_{g,w} + \gamma_{s,w} \cdot dA_{s,w} - \gamma_{s,g} \cdot |dA_{s,g}| = 0. \quad \text{(S14)}$$

(v) Boundary condition: The volume of the water phase, V, do not change.

$$dV = 0. \quad \text{(S15)}$$

With (S11) and (S15) we obtain:

$$\delta\theta = -2/3 \cdot \theta/r \cdot \delta r. \quad \text{(S16)}$$

(vi) We consider the geometry of a 2D-circular cap and calculate the changes of the interfaces (z-dimension is not considered, i.e. one has to multiply each expression by z_0 to obtain the right dimension):

$$dA_{g,w} = 2/3 \cdot \theta \cdot \delta r,$$

$$dA_{s,w} = (2 \cdot \sin(\theta) - 4/3 \cdot \theta \cdot \cos(\theta)) \cdot \delta r = B(\theta) \cdot \delta r . \quad \text{(S17)}$$

(vii) Inserting of (S17) into (S14) yields the following implicite equation for the contact angle in thermodynamic equilbrium:

$$\theta - \frac{3}{2} \cdot \beta \cdot B(\theta) = 0, \quad \text{(S18)}$$

where B(θ) is defined in Eq.(S17) and where we have introduced the wetting parameter

$$\beta = \frac{\omega}{\gamma_{g,w}} , \quad \text{(S19)}$$

with $\omega = \gamma_{s,g} - \gamma_{sw}$. In Fig. S3 we show the sensitive dependency of the contact angle on the wetting parameter β for partial wetting, i.e. for $0 \leq \theta \leq 90°$.

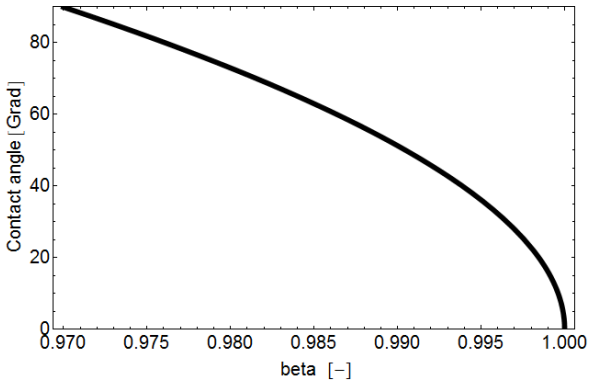

Figure S3 Contact angle versus wetting parameter β.

Complete wetting occurs, if β ≥ 1, i.e. the radius tends to infinity according to

$$r(\theta) = \sqrt{\frac{r_0^2}{(2\theta - \sin(2\theta))}}, \qquad \text{(S20)}$$

with $r_0 = r(\pi/2)$.

(viii) Under the assumption that the interaction of gas molecules with the solid surface is of similar order of magnitude as the interaction of NAPL-molecules (like Toluene; see Pan et al., 2007) with the solid surface, we can consider ω as constant or at least as a small increasing function compared to $\gamma_{NAPL,w} = \gamma_{g,w} - \gamma_{g,NAPL} \approx (73 - 29)$ mN/m. Therefore, we obtain a larger β-value and a according to Fig. S3 a smaller contact angle. Since the area of the fluid-fluid interface is inverse proportial to the contact angle, we anticipate a larger interfacial area for the gas-water system as for the NAPL-water system, i.e. the NAPL-w-interface will extend more than the g-w-interface in thermodynamic equilibrium.

S3: Complete histogram with noisy voxels (Voxel-Nr: 1 -10) for experiment 7.

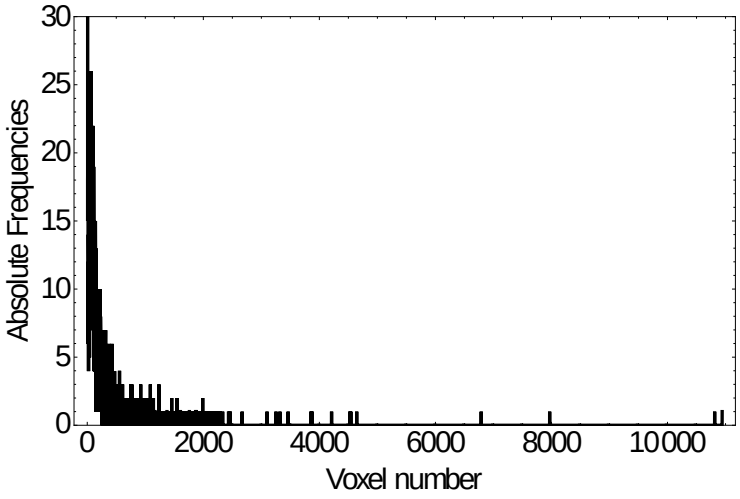

Figure S4 Histogram of unique objects (gas cluster with a certain voxel number) for experiment 7.

S4 Cluster statistics, bubble-size distribution, and pore-size distribution for 2nd series of experiments (3 experiments under same WT-rise)

Cluster statistics

Table S1 Cluster statistics (sp – single-pore trapped gas bubbles with $r_b < r_{k,max}$; mp – multipore-trapped gas bubbles with $r_{k,max} < r_b < r_k$; and l – large trapped gas bubbles; N – number of bubbles; V – gas volume).

Experiment	N_{tot}	N_{sp} [%]	N_{mp} [%]	N_l [%]	V_{sp} [%]	V_{mp} [%]	V_l [%]
7	3695	53	37	10	16	40	44
8	3687	51	38	11	16	42	42
9	4445	50	38	12	12	35	53

Bubble-size distribution

Table S2 LogNormal-Bubble-size distribution: Mean bubble radius and SDV.

Experiment	**Mean radius** [mm]	**SDV** [mm]
7	0.24	0.07
8	0.24	0.07
9	0.23	0.08

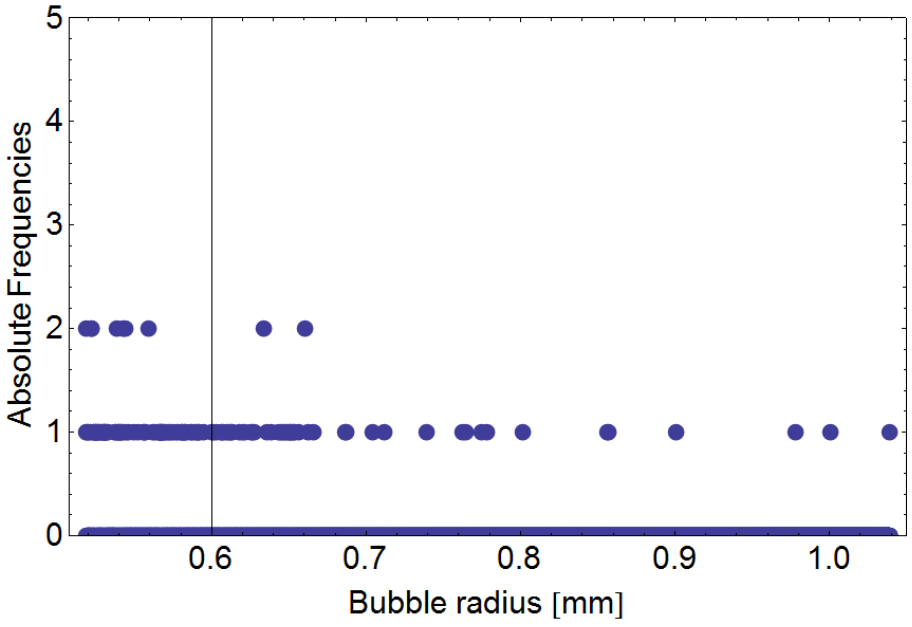

Figure S5 Bubble-size distribution for $r_b > r_k$ (experiment 7).

In Figure S5 the bubble-size distribution is shown for larger bubble radii $r_b > r_k$. Up to r_b = 0.65mm the distribution is nearly uniform; and then rather sparse with only 14 trapped gas bubbles.

Pore-size distribution

Table S3 Pore-size distribution. Mean radius and SDV for the Normal (column 2 and 3) and the LogNormal (column 4 and 5) pore-size distribution.

Experiment	Mean [mm]	SDV [mm]	Mean [mm]	SDV [mm]
7	0.162	0.057	0.175	0.063
8	0.167	0.060	0.181	0.063
9	0.170	0.060	0.181	0.063

S5 Experimental verification of static bubble distribution

In order to proof that the trapped gas phase is static and will not dissolved during the experiment, we conduct an experiment for a 0.7mm-GBS (d_{50} = 0.7mm, packing density 1.56 g/mL, porosity = 0.37) for a WT-velocity of 0.5 cm/min that is equal to that of the second experimental series (exp. 7 -9). The CT-images were taken after 3 different times, 20 min, 3h, and 24 h. The evaluated quantities are listed in Table S4.

Table S4 Porosity, volumetric gas content, total surface and gas-water for 3 different times after WT-rise.

Time	Porosity [-]	Error# [%]	Gas content [-]	a_g [1/mm]	a_{gw} [1/mm]
20 min	0.386	4	0.0136	0.170	0.161
3 h	0.387	5	0.0138	0.165	0.156
24 h	0.385	4	0.0136	0.171	0.161

S6 Histogram of the whole origial imgae of experiment 7.

Fig. S5 shows the complete tri-modal histogram of the original image of experiment 7 indicating the different phases and the threshold pairs ($t_{1g,w}$, $t_{2g,w}$) and ($t_{1w,s}$, $t_{2w,s}$) for segmentation of the gas phase and water phase and the water phase and the solid phase, respectively.

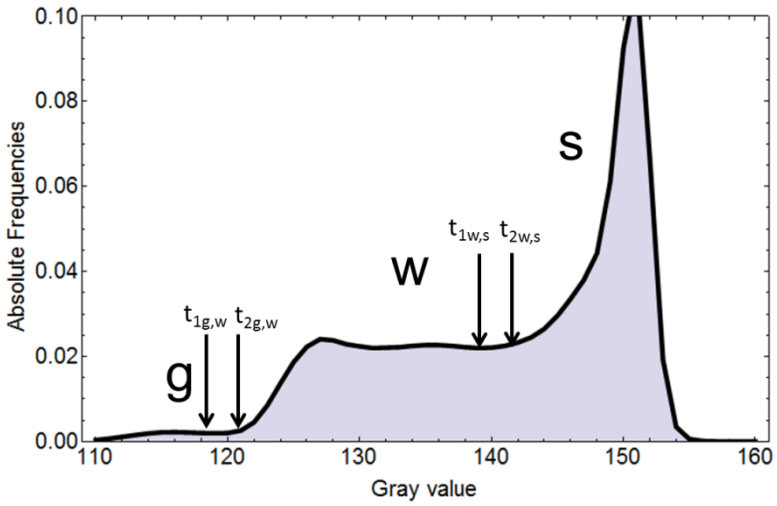

Figure S6 Historgram of the complete CT-image of experiment 7.